JOURNAL OF MATERIALS SCIENCE 18 (1983) 741–752

Microelectronic and medical applications of an ion beam milling system

ZBIGNIEW W. KOWALSKI, IWAJLO W. RANGELOW
Technical University of Wroclaw, 50-370 Wroclaw, Poland

An ion beam milling system utilizing a Kaufman-type source to etch patterns in conductive, semiconductive and insulating materials was used to examine the surface morphology of resistive thick films, and to modify the surface topography of biomaterials. The ion beam sputter modification of the different materials presently used or under consideration for electronic and implant devices were studied. A Japan Electron Optics Laboratory, model JSM-35 scanning electron microscope was used to examine all the materials tested.

1. Introduction

Ion milling is an etching technique utilizing an ion beam to etch (sputter) patterns in electronic devices. The etch rate is dependent upon the type of material sputtered, the angle of ion beam incidence, the ion energy, the type of gas utilized as the ion source, etc. Ions produced in the low pressure (10^{-1} to 10^{-2} Pa) discharge or plasma chamber are extracted, focused and accelerated through optically aligned grids towards the sample holder (target) in a collimated beam with sufficient energy to remove surface atoms. The major advantages of the ion beam etching technique are related to its capabilities in fabricating fine geometry devices. With conventional wet-chemical etchants, it is impossible to prepare lines less than 1 μm wide in a 1 μm thick film (1 : 1 depth to width ratio) and in most cases, chemical etching is limited to spaces of the order of 2 to 4 μm. The ion beam etching is limited in line widths only by the masking capabilities. It is worth mentioning some advantages of the ion beam milling process:

(a) ion beam milling permits repeatable etching of line patterns with dimensions as small as 0.2 μm,

(b) the process has the ability to reliably produce 10 to 1 depth to width ratio channels without undercutting,

(c) etch channel walls can be held to vertical configurations or given precise tapers up to 0.785 rad (45°),

(d) a fully collimated ion beam can eliminate undesirable etching effects such as "ears" and "trenching",

(e) low ion beam energies can eliminate radiation damage,

(f) ion beam milling permits the etching of virtually any material to precise depths and geometries by the proper selection of ion beam energy, impact angle and masking,

(g) the water-cooled substrate holder keeps the sample surface temperatures below 373 K (100° C),

(h) the substrate is not immersed in the etching medium (i.e. chemical bath or plasma) but is loaded into a vacuum chamber and exposed to a collimated ion beam.

A new area of potential application for the ion sputtering process is in the field of implantology. The ion bombardment of implants may lead to modifications of the surface morphology and chemistry of the implant materials. In order to develop clinically acceptable materials, the influence of material properties on the biological response must be understood. In the last five years the ion sputtering technique has become widely used in attempts to modify the surface morphology and chemistry of biocompatible materials such as metals, alloys, polymers and ceramics [1–4]. Many experiments were performed to investigate the influence of the ion sputtering of implants on the surface composition

0022–2461/83/030741–12$03.94/0

and mechanical properties of implant materials, surface topography of implants and tissue response in the tissue surrounding the sputtered implant. Ion beam sputtering is potentially useful in the study of the effect of surface morphology on the biological response because of the ability of this technique to control the surface roughness [5]. Results obtained by several authors showed the beneficial effect of ion sputtering on tissue reponse (initial thrombus growth, tissue inflamatory, mechanical attachment of soft tissue to the implant material and/or thrombus to the vascular implant). It has been stated that one of the several factors which affect the biological tissue reponse to an implant material is the surface roughness. The mechanical of how it affects the tissue response are not understood.

The intent of this paper is to give the major information about the design, parameters and operation of the ion beam milling system used for the results reported herein and to describe the microelectronic applications (fabricating of the fine geometry devices, preparations of resistive thick films for scanning electron microscopic examinations) and medical applications (altering of the surface topography of biological implant materials) of this apparatus.

2. Apparatus

The ion beam milling system used in the experiment consisted of a source to generate the ion beam, a work chamber in which the ion beam milling occurred, a fixture for holding the sputtered samples in the ion beam and a vacuum system. The ion source based on the Kaufman ion thruster concept developed by NASA, similar to that presented elsewhere [6], was used for the results reported here. The ion beam was extracted from plasma created by a nonsustaining low voltage arc discharge. The discharge was obtained by applying a voltage of about 40 V between an electron-emitting, hot, 0.8 mm diameter tantalum filament cathode and an anode cylinder (discharge chamber) located in the outer diameter of the discharge region. The anode was at the ground potential. To increase the ionization efficiency of the electrons a solenoid magnetic field was applied. The gas to be ionized, usually argon, was introduced to the discharge chamber at a pressure of 10^{-1} to 10^{-2} Pa. To prevent collisional effects, which could cause beam scattering and redeposition, it was necessary to maintain the pressure in the work chamber below 10^{-2} Pa. To provide this differential, argon was bled into the discharge chamber through an adjustable capillary valve and pumped out through the work chamber. The main reasons for selecting argon were: (a) it is inert, (b) has a high mass and (c) it is relatively inexpensive. The ions created in the discharge chamber were extracted and formed into a 5 cm diameter ion beam by a system of two molybdenum grids with precisely aligned slots [7]. The first (screening grid) was connected to the anode and the second (extracting grid) was connected to a drift tube. This 7 cm diameter tube formed the equipotential distribution in the drift region. Use of the drift tube followed from the applied voltage supply. The potential of the extraction grid and sample holder (fixturing) related to the earth potential, was negative (0 to -1000 V). The plasma in the source formed a sheath around the grid slots preventing the field applied between the grids from penetrating into the discharge region. The extracted ions were those that reached the sheath through random thermal motion. Ions crossing the sheath were accelerated by the potential applied between the grids. Neutralization of the beam, important in the sputtering of insulating materials, can be achieved by injecting electrons from a 0.3 mm diameter tantalum filament (not used in the experiment). The neutralizer is mounted between the extraction system and the sample holder. The low energy neutralizing electrons do not participate directly in the milling process, nor do they contribute to the heating of the substrates. The substrate holder was water-cooled to keep the substrates below the critical temperature (about 373 K i.e. 100° C) during the ion sputtering process.

3. Experimental procedures

3.1. Samples

Three types of samples have been investigated:

(a) silicon oriented ⟨1 1 1⟩(n) uncovered and covered with vacuum evaporated chromium/gold layers and with aluminium. Samples were coated with 1 μm thick Shipley AZ1350 resist. Micrometre size line patterns have been developed in the resist using deep ultraviolet (UV) and contact masks. The gold and aluminium layers were 1 μm thick and the thickness of the chromium layer was 0.02 μm,

(b) low-resistivity thick films of NiP and glass

on the alumina substrate, baked in 930 K. The average thickness of these films was 100 μm,

(c) samples of materials for implantation into the human body (artifical bones), now in use (stainless steel, titanium) and under investigation (alumina ceramic). Chrome–nickel stainless steel samples 1.5 cm wide and 3 cm long were cut from a wide plate of type 63018 (OSTEO AG, Selzach products, 1976). This steel (containing 17.5% chromium, 12.5% nickel, 3% molybdenum and 0.03% carbon maximum) used for orthopaedic implants, corresponds to the American standard AISI 316LC or the German material number 4435. Titanium is a good material for dental implants (titanium endosteal blade vent implants). In the experiment polycrystalline 99.98 % titanium was studied. Alumina ceramic is commonly used as substrate material for thick film circuits but recently it has appeared that it could be a satisfactory biological material. Therefore polycrystalline ceramic specimens of 96% fine-grained, sintered alumina in the form of plates 2 cm x 3 cm were also investigated.

3.2. Irradiation

Ion irradiation was performed in an ion beam milling system as described above. All the materials investigated were bombarded at normal incidence by Ar^+ ions at an applied voltage of 500 to 1000 V and at an ion current density up to 2.0 mA cm^{-2} (current measurements taken on stationary ion collector – 49 Faraday cages system, at normal ion incidence). During all sputtering processes the gas to be ionized (argon) was introduced into the discharge chamber at a pressure of about 5×10^{-2} Pa. All the samples were positioned and ion etched (sputtered) for 15 to 90 min (microelectronic materials: gold, aluminium, silicon, NiP + glass) or for 50 to 600 min (biological implant materials: chrome–nickel stainless steel, titanium, alumina) at an ion source–sample distance of about 15 cm.

3.3. Electron microscope observations

All the materials studied were examined using a Japan Electron Optics Laboratory, model JSM-35, scanning electron microscope. Before scanning electron microscope (SEM) observations the alumina ceramic (insulating material) was coated with a thin film of chromium.

4. Results and discussion

4.1. Fabrication of micrometre line patterns

Microelectronic circuit fabrication is based on the ability to selectively remove material from, and to add deposit material to the surface of a suitable substrate.

Ion-beam etching has two additional attributes that commend its use for special device fabrication. Firstly, it is an universal etchant (can etch any material or combinations of materials). Secondly, ion etching consists of shadow masking to expose various surfaces to the beam. Thus, a shadow masked surface does not suffer from etch penetration beneath the masking layer, which leads to mask undercut or tunnel formation. However, the nature of ion etching is such that several unique problems are encountered when the technique is applied directly. The problems encountered with ion-beam etching (sputtering) are namely, mask erosion and faceting [8], redeposition [9] and trenching [10].

Since most microelectronic applications of ion beam etching requires masking to produce relief patterns, care must be taken when choosing masking materials. In the experiment, Shipley AZ1350 resist was used to delineate the structures (patterns), and to enable a detailed study of the sputtered patterns to be carried out. Micrometre size line patterns were developed in the resist using deep UV and contact masks.

A problem encountered with ion sputtering is that backsputtered material tends to redeposit around the edges of steep surface features [9]. Redeposition is often observed along the edges of photoresist patterns, where ridges of material are left behind when the resist pattern is removed [10].

The development of "trenches" (see Fig. 1) around the base of the mask edges is another result which is often observed when ion etching is applied. Their appearance can be easily explained by the fact that, as the mask is faceted ions incident on the sidewall are reflected down towards the base of the pattern. Thus, the mechanism is subjected to an increased ion flux density that causes a more rapid erosion, and a stable trench feature develops. As stated earlier, the facet angle corresponds to the angle of maximum etch rate. If it was possible to shift the maximum etch rate from the typical 35 to 65° angle (0.61 to 1.13 rad) of ion bombardment to 0°, no facet

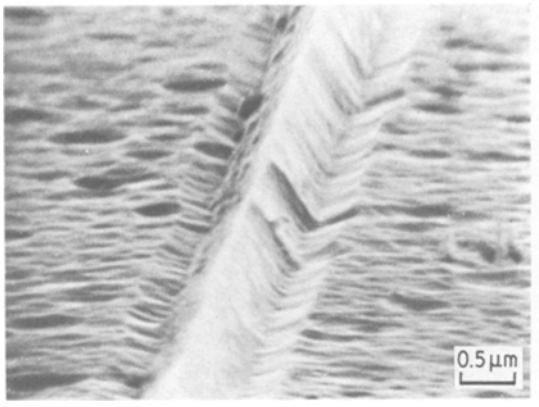

Figure 1 Trenches developed at the bottom of the line pattern after 20 min of ion sputtering of 1 μm aluminium thin film. Accelerating voltage of 500 V and ion current density of about 0.5 mA cm^{-2}.

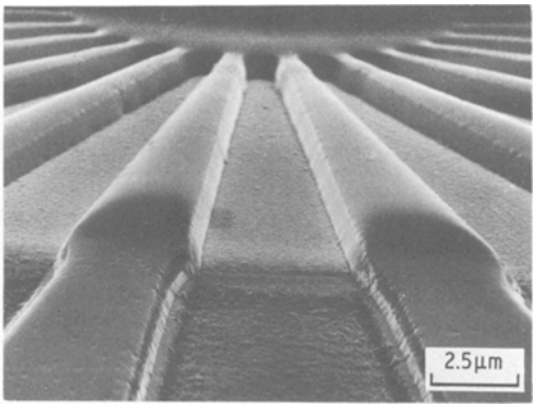

Figure 3 Scanning electron photomicrograph of unsputtered (screened during ion irradiation) and sputtered gold line patterns with AZ1350 resist still in place (lower part of the image). Accelerating voltage of 1000 V and ion current density of about 0.25 mA cm^{-2}.

would be formed and desirable features would be produced: etched lines with nearly vertical walls and a flat base (no trenching would occur at the base of etched lines [10, 11]). A reduction of trenching can be achieved by increasing the tilt angle to a value greater than $\pi/2$ rad minus the slope of the sidewall.

Etching uniformity is a very important parameter in fine pattern fabrication by ion beam sputtering of various pattern sizes. Patterns with different sizes have different wall slopes. The ion etching is strongly dependent on the angle of ion beam incidence. Therefore, the change of pattern size will be different for patterns with different sizes. Fig. 2 shows the correlation between theoretical and experimental results, presenting a relationship between the changes of pattern size and pattern wall slope for an AZ1350 photoresist mask layer on a thin film of gold. The change of size, p, can be calculated from the relation

$$p = \frac{V(\theta_w)}{\sin \theta_w} \qquad (1)$$

where θ_w is the slope of pattern wall, $V(\theta_w)$ is the etch rate of the slope (measured on the pattern wall). To compare the pattern sizes and the slope of the pattern walls of the material sputtered with the initial one, the double layer of chromium/gold on silicon oriented ⟨1 1 1⟩(n) substrate was partially screened by molybdenum foil within the bombarded surface area. A scanning electron photomicrograph of gold line patterns with AZ1350 resist still in place, sputtered with a screen mask is presented in Fig. 3. Information about the changes of pattern size and about the slope of the pattern walls can be made from the substrate cross-section perpendicular to the strip direction. The cross-section was prepared by breaking the substrate after scratching with a diamond. Small geometry patterns with line widths of 1 μm or less, fabricated by ion beam milling, were correct when the slopes of the pattern walls were in the range 70 to 90° (1.22 to about 1.57 rad). Fig. 4 shows patterns etched in silicon oriented ⟨1 1 1⟩(n) substrate. The slope of the walls was about 70° (1.22 rad). The change of sizes was small because the etch rate of the slopes was minimal. The changes in pattern widths were less than 10%. The widths of the patterns milled in silicon were 0.25 μm (Fig. 4a) and 0.6 μm (Fig. 4b), respectively.

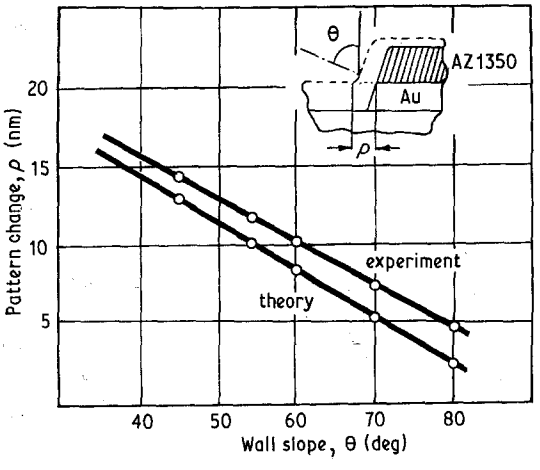

Figure 2 Pattern size, p, as a function of pattern wall slope θ_w for Cr/Au on silicon substrate.

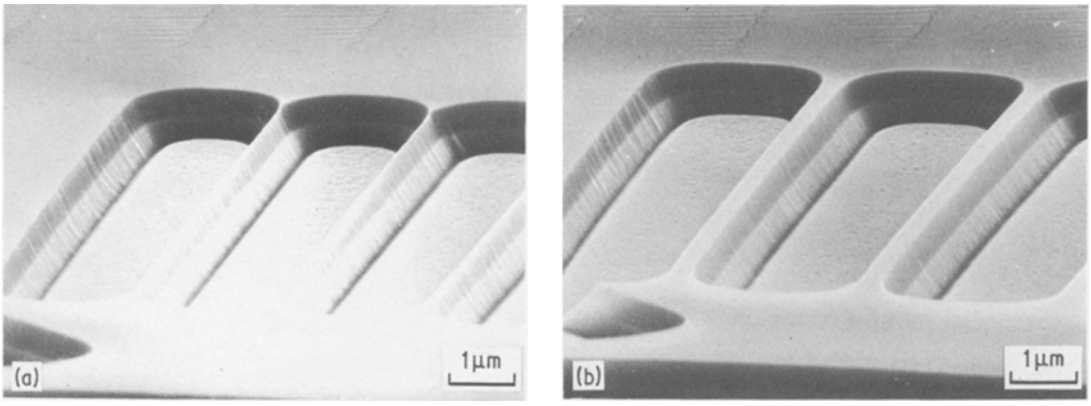

Figure 4 SEM images of fine geometry patterns milled on ⟨111⟩ silicon substrate with AZ1350 resist still in place. Accelerating voltage of 500 V and ion current density of about 1 mA cm^{-2}. Widths of line patterns of about, (a) 0.25 μm and (b) 0.6 μm.

When the ion sputtering (milling) was carried out with a single mask layer, the patterns were not uniformly etched because of the patterned wall slope effect.

4.2. Examination of the surface morphology of thick films

The ion beam etching (sputtering) method of protruding texture in the thick layer, under discussion, has been used already [12–15] for the examination of metallographic samples. This is a dry method which enables selective removal of various materials. The etching process can be realized over a precisely selected area and it may be stopped at any time. The temperature of the sputtered sample surface did not exceed 330 K. The main factor which determined the shapes of the characteristic formations on the etched surface was the dependence of sputtering yield $S(\theta)$ on the angle of the beam incidences θ and on the composition of the etched material. As the time of ion beam sputtering was prolonged, the surface of a fine-grained sample revealed more and more cones with apex angle α_0. The value of this angle was characteristic for the material asperity. It has been proved experimentally and analytically [14] that

$$\alpha_0 = \pi - 2\theta_m \qquad (2)$$

where θ_m is the angle of ion beam incidence by which sputtering yield becomes maximum.

The possibility of analysis of a thick film microstructure using the surface morphology dependence on etching time has been investigated with NiP and a glass composition, baked at 930 K. Fig. 5 presents the sample surface before (Fig. 5a) and after 30 and 90 min of ion beam sputtering. An argon beam with a current density of 0.5 mA cm^{-2} and an accelerated potential of 500 V was applied. First the erosion of the component having a higher etching rate occured, and the layer of NiP was removed (Fig. 5b). Then glass "grains" were etched. Cones began to develop when surfaces (planes) with the angle θ_m to the ion beam were exposed to the beam.

The ion beam sputtering process appeared to be a suitable method of texturing inhomogeneous materials. It did not cause mechanical deformation of the microstructure. The sample was heated no higher than 300 K. A strong dependence of sputtering yield on the ion beam angle of incidence and on the etched material caused differential of the morphology of sample surface (Fig. 6), especially for samples composed of various materials [15].

4.3. Modification of surface morphology of biological implant materials

Ion beam etching as a potentially useful roughening technique can be utilized in attempts to modify the surface topography of biocompatible materials. To obtain surface roughness or controlled surface topography three different ion sputtering techniques can be used.

(a) Natural sputtering (properly: natural texturing, i.e. microroughening of the bombarded surface of the sample that occurs if there are spatial variations in the sputtering yield of the target surface).

(b) Sputtering with a sputter resistant material, seed material, supplying surfaces during the ion sputtering process, i.e. seed texturing.

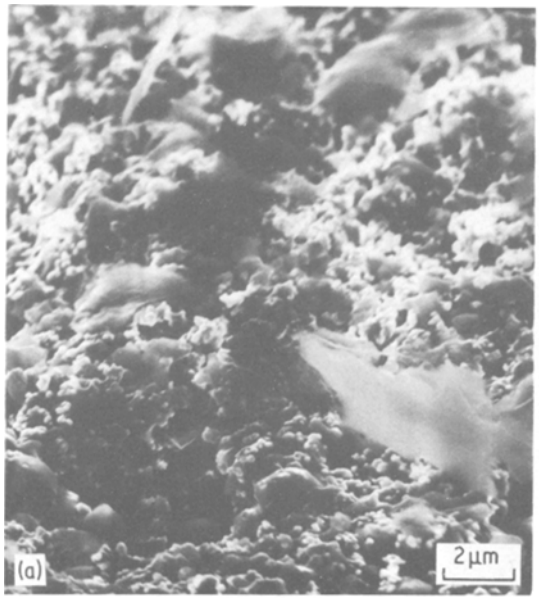

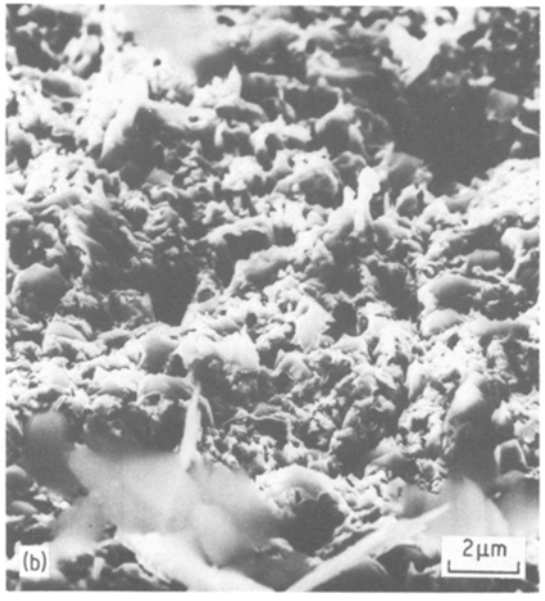

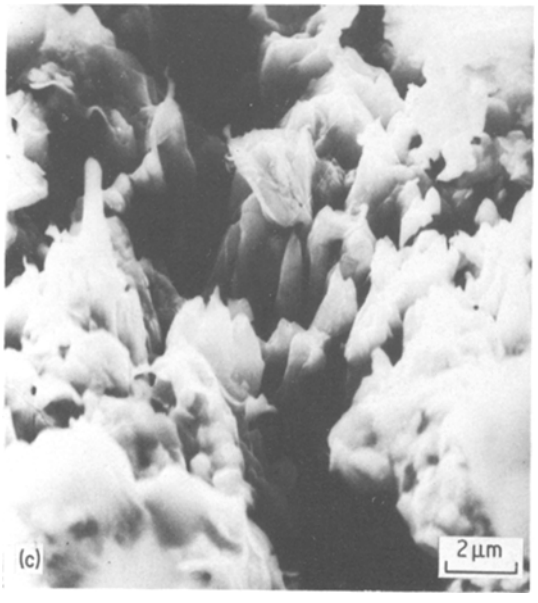

Figure 5 SEM photomicrographs of the surface of low-resistivity thick film of NiP and glass. (a) Before ion sputtering and after, (b) 30 min of ion irradiation and (c) 90 min of ion bombardment.

(c) Sputtering through a screen mesh masks superimposed on the material during ion sputtering. The screen prevents the erosion of the material directly beneath it, resulting in a surface with an array of pores of constant dimension.

Associated with both the screen mesh mask and the seeding techniques to alter the surface morphology, there was some contamination of the target material by the mesh or seed material. This was partially removed by further sputtering after the mesh or seed was removed.

Chrome–nickel stainless steel mainly used for orthopaedic implants was natural sputtered and sputtered through the stainless steel screen mesh

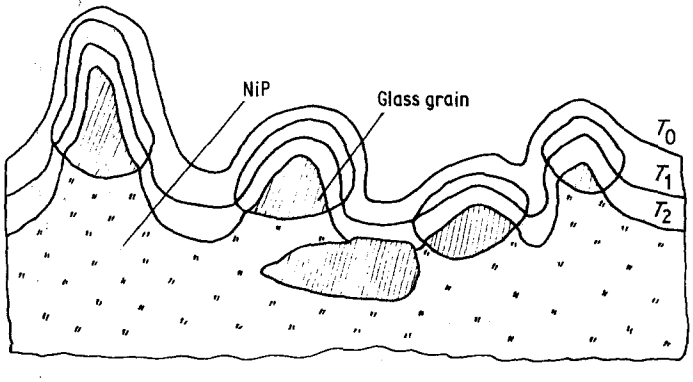

Figure 6 The mechanism of ion beam sputtering (texturing) of inhomogeneous materials [15].

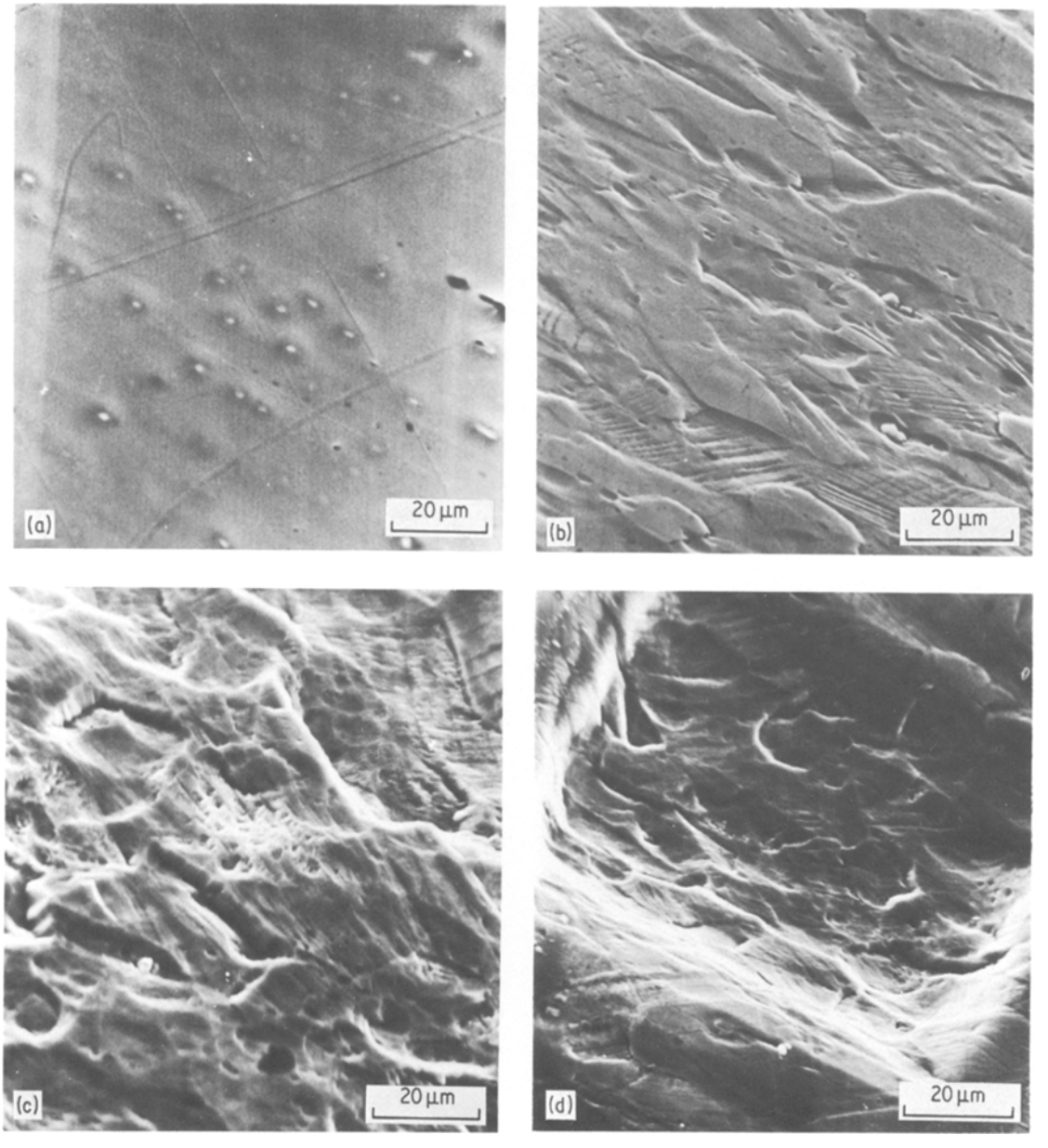

Figure 7 Scanning electron photomicrographs of chrome–nickel stainless steel, (a) before ion irradiation, (b) after natural texturing for 50 min at an accelerating voltage of 1000 V and beam current density of about 1 mA cm^{-2}, (c) after natural texturing for 600 min at the same voltage and beam current density of 0.8 mA cm^{-2} and (d) after 210 min of sputtering through the stainless steel screen mesh mask (1000 V, 2 mA cm^{-2}).

mask for 50 to 600 min. The results of ion beam bombardment of chrome–nickel stainless steel specimens are illustrated in Fig. 7. Fig. 7a shows a SEM image of the stainless steel surface before ion irradiation. SEM photomicrographs of the surfaces after ion sputtering are shown in Fig. 7b (natural sputtering for 50 min), Fig. 7c (natural sputtering for 600 min) and Fig. 7d (sputtering through the screen mesh mask for 210 min). The unsputtered surface was almost smooth. Only a few pits with inclusions of grinding compound and some flows, after polishing, could be observed. After ion bombardment the initial smooth surface changed with a tendency to roughening. The ion sputtered surface became more textured, the surface topography was distinctly visible, and the

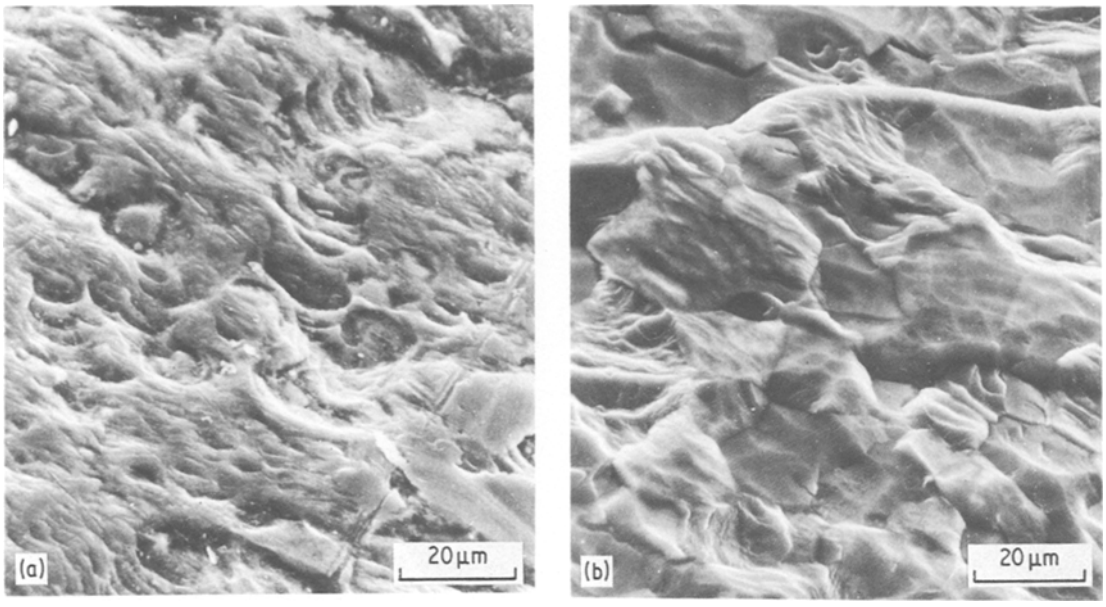

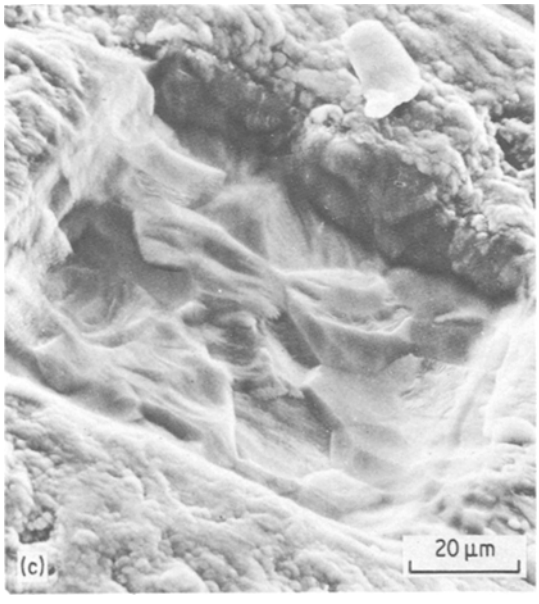

Figure 8 Titanium surface topography before and after 210 min of ion beam sputtering at an accelerating voltage of 1000 V and beam current density of 2 mA cm^{-2}, (a) before ion bombardment, (b) after natural texturing and (c) after sputtering through the stainless steel screen mesh mask.

surface roughness increased as the ion sputtering duration increased (see Figs. 7b and c). Roughening was determined as occurring independently of the ion sputtering technique used in the experiment. The surface topography of stainless steel sputtered through the screen mesh mask observed at the bottom of the pit (see Fig. 7d) was similar to that obtained by 600 min natural sputtering.

Titanium, a material used for dental implants, was also ion etched to obtain larger roughness or controlled surface topography. Fig. 8 shows scanning electron photomicrographs of the titanium surface before (Fig. 8a) and after ion beam sputtering (Figs. 8b and c). Fig. 8b presents the titanium surface after natural texturing for 210 min and Fig. 8c illustrates the surface after sputtering through the stainless steel screen mesh mask imposed on the titanium sample (for the same time). The initial, unsputtered surface was altered during the ion bombardment with an inclination to creating larger topographical features. To compare the bombarded surface topography with the initial one it is convenient to observe the sample after irradiation through the screen mask (Fig. 8c). On one photomicrograph two regions can be observed: sputtered region at the bottom of the etched pit and the unsputtered one, shielded during ion bombardment by the screen mesh mask. The surface topography of ion etched titanium at the bottom of the pit was similar to that observed after natural sputtering. SEM image of alumina surface after 210 min of ion beam etching through the stainless steel screen mesh mask imposed on the target is shown in Fig. 9. The surface topography of sputtered alumina observed at the bottom of the etched pit was not "typical". The topography obtained usually after natural sputtering [5] or/and sputter-

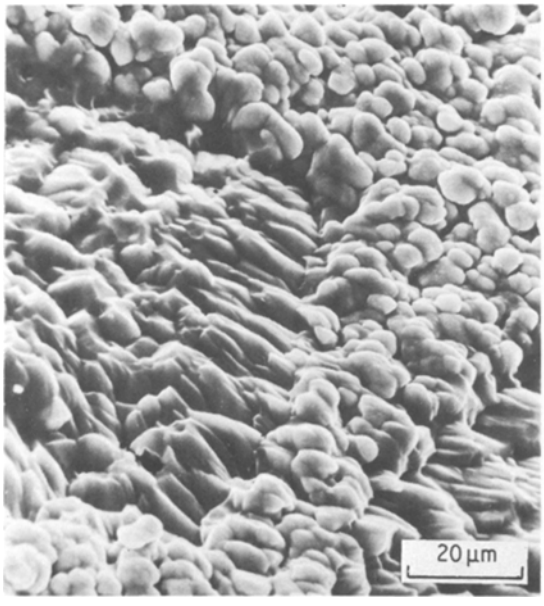

Figure 9 SEM image of alumina surface topography resulting from 1000 V Ar^+ ions sputtering through the screen mesh mask for 210 min, beam current density of about 2 mA cm^{-2}.

ing through the screen mesh [3] was similar to that presented in Fig. 10. The initial topography changed with a tendency to smoothing but simul-

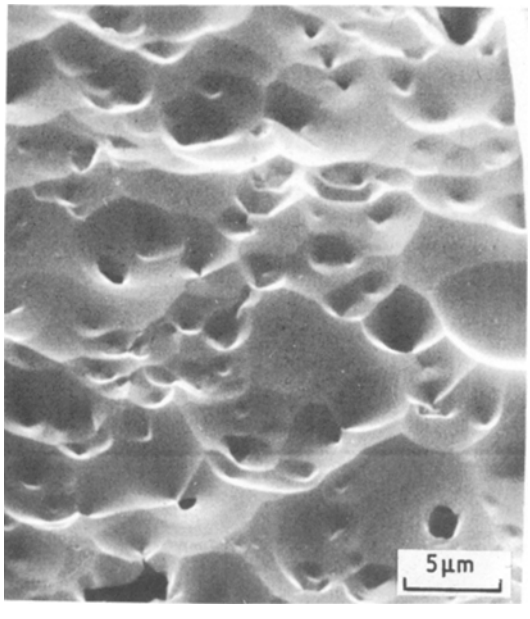

Figure 10 Characteristic surface topography of alumina usually observed after natural texturing [3], [5]. Presented topography was obtained after ion beam irradiation from the hollow anode source with glow discharge. Accelerating voltage of 7 kV and beam current density of about 0.5 mA cm^{-2}.

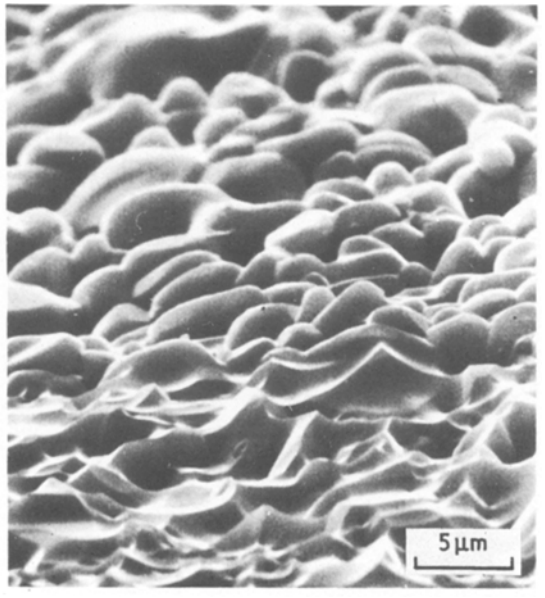

Figure 11 Border between unsputtered (upper part) and natural textured (lower part) alumina surface obtained by Ar^+ ions irradiation from the hollow anode source [5].

taneously roughening occurs due to preferential sputtering of the pore wealls. Both these processes determine the final state of the surface topography. Grains and grain boundaries observed before ion beam bombardment were not seen after ion irradiation. The sputtering process can be considered as the erosion of the ion impact amor-

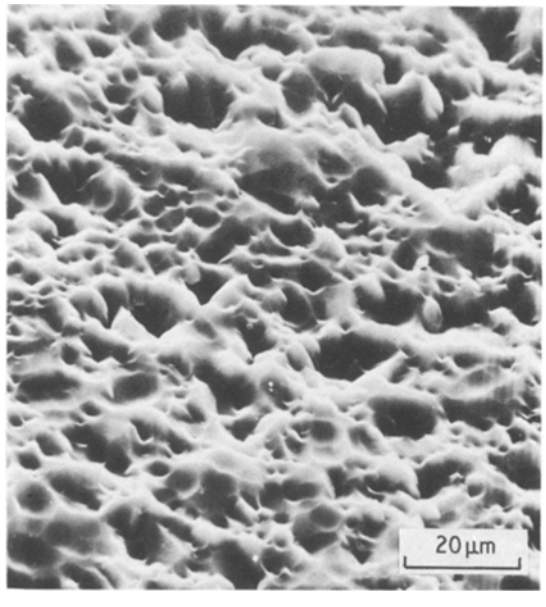

Figure 12 SEM photomicrograph of alumina surface after 90 min of ion beam sputtering with tungsten seed (tungsten seed texturing) [17].

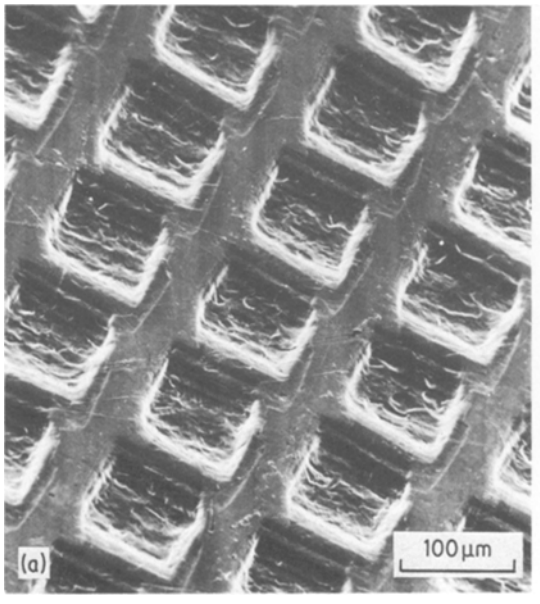

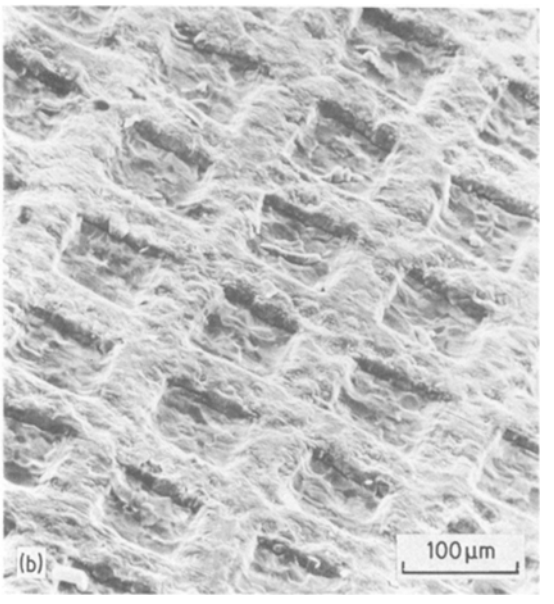

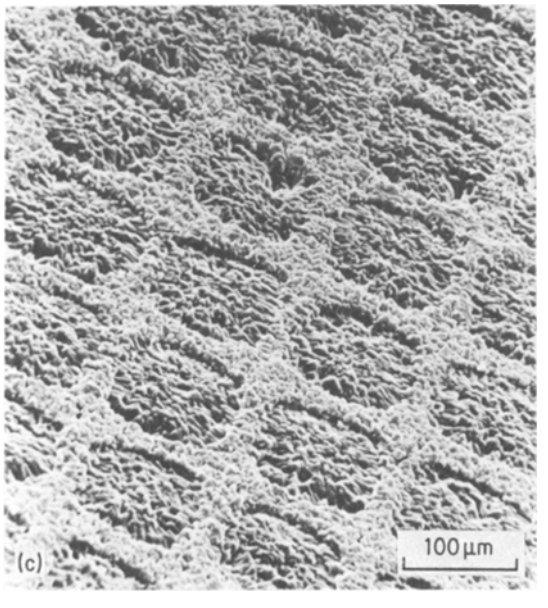

Figure 13 Pitted surfaces of three different materials presently used or under consideration for implant devices resulting from 210 min of ion beam sputtering through the stainless steel screen mesh mask, (a) chrome–nickel stainless steel, (b) titanium and (c) alumina.

phized homogeneous and isotropic material containing pores and inclusions [16]. The mechanism of ion beam sputtering of alumina described above was independent of the sputtering conditions used in the experiment. The topographies similar to that presented in Fig. 10 were obtained both for natural sputtering by argon ions at an applied voltage of 7 kV, ion current density of about 0.5 mA cm^{-2} and an ion source–biomaterial distance of about 1.5 cm [5] and for sputtering through the screen mesh mask by argon ions with energy of 1750 eV, ion current density of 0.4 mA cm^{-2} and 20 cm distance between the source and biomaterial [3]. This characteristic surface topography of alumina was observed even if the sputtering rate was minimal i.e. when a thickness of material layer removed by sputtering was too small to measure it. To measure the removed material thickness and to compare the bombarded alumina surface topography with the initial one the surface of the alumina sample was partially screened with molybdenum foil during the ion beam sputtering. The border (boundary) between the screened surface and the sputtered area is shown in Fig. 11. The initial surface is seen in the upper part of the image and the sputtered one, with characteristic topography and similar to that presented in Fig. 10, is shown in the lower part of the photomicrograph.

As yet, no unambiguous explanation of the mechanism of creating of the alumina surface topography at the bottom of the sputtered pit presented in Fig. 9 has been provided. Possible reasons could be considered.

(a) Irregular sputtering of the pit due to the local repelling and distorting of the ion beam. In the central region of the pit the surface probably becomes positively charged, whereas in the vicinity

TABLE I Etch rates of materials studied for normal argon ion beam incidence. Etch rates for different ion current densities and different energies may be estimated from the etch rates being proportional to ion beam current density and approximately proportional to energy (in the 500 to 1000 eV range)

Material	Etch rate (nm min^{-1})				
	1 mA cm^{-2}				2 mA cm^{-2}
	500 eV*	500 eV†	700 V‡	500 V§	1000 V§
Alumina	10	8–12	18	–	50–70
Aluminium	52	31–66	69	50	–
Gold	140	100–145	185	145	–
Resist AZ1350	–	20–25	26	30	–
Silicon	37	22–38	41	40	–
Stainless steel 304 or 316	25	25	–	–	140 max
Titanium	32	13–35	22	–	95 max

*1979 Veeco Catalog, p. T 22, Table I,
†B. A. Banks, NASA TM-81721, 1981,
‡Technics Catalog, MIM-TLA 12,5, 5/80, 241,
§ our experiment,
– no data.

of the screen mesh mask there is a great number of electrons (secondary electrons from the mask) which prevents the surface charging. It is probably the main reason for deeper etching of the pit in the vicinity of the screen mesh mask.

(b) Supplying the alumina surface with low sputtering yield atoms of stainless steel screen mesh mask (seed material) during ion sputtering process. The surface topography observed in Fig. 9 is similar to that obtained elsewhere [17] by tungsten seed texturing (see Fig. 12).

(c) Applying lower accelerating voltages in comparison with voltages (or energies) used elsewhere [3, 5].

In the last five years the ion beam sputtering through the screen mesh masks has become widely used in attempts to modify the surface morphology of biological implant materials. Many experiments were performed to investigate the influence of the pitted surface topography (obtained by ion beam sputtering through the screen mesh mask) on such problems as:

(a) changes in the healing process that result from the presence of an implant,

(b) a tissue inflamatory and/or foreign body response in the tissue surrounding the implant,

(c) a firm attachment of the surrounding tissue to the implant material.

As yet, it is difficult to say anything definite about the clinical performances or mechanical retention of the implants sputtered through the screen mesh masks. The results obtained after implantation of sputtered orthopaedic and dental implants indicates no statistically significant differences between bone–implant interfacial shear strengths of sputtered and smooth (unsputtered) implants [4]. However, *in vivo* ageing increased the mechanical strength of the sputtered implants and reduced that of the smooth implants.

The application of pitted surface structures to direct ingrowth orthopaedic and dental implants will require additional knowledge of the short and long term consequences. Recently the ion beam sputtering has been used in conjunction with the screen mask to produce polytetrafluoroethylene tubes with many small apertures. The perforated catheter implanted in one of the lateral ventricles of the brain is applied for treatment of hydrocephalus [4].

In our experiment chrome–nickel stainless steel, titanium and alumina, the materials presently used or under consideration for implant devices were ion beam sputtered (using an ion beam milling system) through the stainless steel screen mesh masks. Scanning electron photomicrographs of the pitted surfraces of these materials obtained after ion irradiation for 210 min are shown in Fig. 13. Although the time of ion bombardment was the same for each material, the depths of the sputtered pits observed in Figs. 13a, b and c are different. It depends on etch rates of materials sputtered. The etch rates of materials studied, for normal argon ion beam incidence, in comparison with results obtained elwewhere are listed in Table I.

5. Conclusions

The ion beam milling system has proved to be a valuable tool not only in the fabrication of high resolution microelectronic devices but also in the examination of the surface morphology of thick films and in the preparation of surfaces of biological implant materials. Ion beam milling permits the etching of virtually any material to precise depths and geometries by the proper selection of ion beam energy, impact angle, and masking. SEM observations of the low-resistivity thick films after ion beam milling enable the estimation of the composition of grains and the examination of the surface texture. Ion beam sputtering can microscopically roughen the surfaces of implants and/or modify the surface topographies of implants in a controlled manner. The feasibility of this method was confirmed by microscopic examination. The resulting surface topography may be used potentially to improve the biological response to implant materials.

Acknowledgements

We are much indebted to Mrs W. Nowak and Dr S. Smardz for their help in the experimental work. We would like to thank Dr W. Czarczyński for the helpful cooperation.

References

1. B. A. BANKS, A. J. WEIGAND, CH. A. BABBUSH and C. L. VAN KAMPEN, NASA TM X-73512, 1976.
2. A. J. WEIGAND, M. L. MEYER and J. S. LING, NASA TM X-3553 (1977).
3. A. J. WEIGAND, NASA TM X-78851 (1978).
4. B. A. BANKS, NASA TM 81721 (1981).
5. Z. W. KOWALSKI, *J. Mater. Sci.* **17** (1982) 1627.
6. Polish Patent No 224669 (1980).
7. I. W. RANGELOW, The 8th International Conference on Plasma Science, Sante Fe, New Mexico, May, 1981.
8. M. CANTAGREL, *J. Vac. Sci. Technol.* **12** (1975) 1340.
9. G. GLOERSEN, *Solid State Technol.* (1976) 68.
10. R. LEE, *J. Vac. Sci. Technol.* **16** (1979) 164.
11. S. SOMEKH, *ibid.* **12** (1975) 28.
12. R. S. BERG, G. J. KOMINIAK, *ibid.* **13** (1976) 403.
13. W. R. HUDSON, *ibid.* **14** (1977) 286.
14. M. J. WITCOMB, *J. Mater. Sci.* **9** (1974) 1227.
15. A. DARLINSKI and I. W. RANGELOW, "26 Intern. Wiss. Koll.", Heft 6, Vortragsreihen B2, B3, B4 (Technische Hoschule Ilmenau, DDR, 1981.) p. 67.
16. M. LUKASZEWICZ and W. HAUFFE, Proceedings of the Conference on Electron Technology, Science Papers of IET of Wrocław Technical University No. 24, Conferences No. 4 (Wyd. Pol. Wrocł., Wrocław, 1980) p. 234.
17. Z. W. KOWALSKI, *J. Mater. Sci.* **17** (1982) 2599.

Received 6 May
and accepted 16 July 1982